The {Bis-2,6-[1-(2-imidazol-4-ylethylimino)ethyl]pyridine}copper(I) Cation. A Synthetic Cu^{I} Oxygen Carrier in Solution as a Potential Model for Oxyhemocyanin †

By **Miriam G. Simmons, Connie L. Merrill,** and **Lon J. Wilson,*** Department of Chemistry, William Marsh Rice University, Houston, Texas 77001
Lawrence A. Bottomley and **Karl M. Kadish,*** Department of Chemistry, University of Houston, Houston, Texas 77004

The red copper(I) title compound $\{[Cu^{I}(imep)]^{+}\}$ is apparently the first synthetic copper complex to functionally mimic hemocyanin in its capacity to reversibly bind O_2 in solution under ambient conditions (1 atm O_2; room temperature) with a reversibility factor of *ca.* 80% per oxy/deoxy cycle. Manometry has established the O_2 : Cu reaction stoicheiometry to be the same (1 : 2) as for the oxygenation of hemocyanin. The green oxy form of $[Cu^{I}(imep)]^{+}$ is proposed to be a μ-dioxygen species with each CuN_3O centre of the binuclear unit being six-co-ordinate and having two imidazole, one pyridine, and two imine nitrogen-donor atoms. Like oxyhemocyanin, the oxy form of $[Cu^{I}(imep)]^{+}$ is essentially e.s.r. silent at 100 K, indicating a fully coupled $S = 0$ ground state if the binuclear centre is formally viewed as $[Cu^{II}-O_2^{-2}-Cu^{II}]$. However, unlike hemocyanin, the $[Cu^{I}(imep)]^{+}$ cation does not form an adduct with CO under ambient conditions. If the imidazole moieties are replaced by pyridine groups, $[Cu^{I}(pyep)]^{+}$, the copper(I) centre no longer reversibly binds O_2. This result is consistent with cyclic voltammetric data showing the Cu^{I} state for $[Cu^{I}(pyep)]^{+}$ to be stabilized by 130 mV relative to that of $[Cu^{I}(imep)]^{+}$. Cyclic voltammetry has also been used as a probe for observing and following what is presumed to be the reversible oxygenation process of $[Cu^{I}(imep)]^{+}$ and to demonstrate the lack of reactivity with CO. Finally, the $[M(imep)][ClO_4]_2$ and $[M(pyep)][ClO_4]_2$ (M = Cu^{II} or Zn^{II}) compounds have been isolated and characterized for purposes of comparison with their Cu^{I} analogue.

AMONG the O_2-transport metalloproteins, only iron and copper are known with certainty to serve at the active site, with iron being present in hemoglobin, erythrocruorin, chlorocruorin, and hemerythrin and copper occurring in hemocyanin. For the hemoglobins, both the nature of the Fe–O_2 bonding and the stereochemistry of the Fe(heme)–O_2 centre have been reasonably well documented.[1] The other O_2-transport proteins have not been as exhaustively characterized and only incomplete information is available.

In probing the structure and nature of the active site, an alternative to directly studying the protein is to synthesize, by design, small molecule compounds which accurately mimic the desired protein function. For the O_2-transport proteins, Collman's 'picket fence' porphyrin model [2,‡] for the iron centre in hemoglobin stands as the most notable achievement to date of this approach. However, for non-heme protein cases like hemerythrin and hemocyanin, where there exists no well defined prosthetic group outside the protein and where the gross structural features of the active site are still in question, the modelling approach looms as even more of a challenge.

Hemocyanin (hcy) from *Helix pomatia* (*M ca.* 9×10^6) is the largest of the hemocyanins, containing *ca.* 300 coppers per protein unit. This size accounts for the difficulty in crystallizing the hemocyanins and insures that no detailed single-crystal *X*-ray structural information about the active site will soon be forthcoming. However, in a recent EXAFS § study of keyhole limpet (*Megathura crenulata*) hemocyanin,[3] it has been concluded that: (i) all the copper in oxyhcy is best formulated as Cu^{II} and in deoxyhcy as Cu^{I}, (ii) contrary to some spectral evidence,[4] sulphur is not present in the primary co-ordination sphere about copper in either form, and (iii) there are three or four oxygen and/or nitrogen donor atoms in deoxyhcy and five or six such atoms in oxyhcy. Furthermore, the reaction stoicheiometry (O_2 : Cu, 1 : 2),[5] the diamagnetism,[6] and the resonance Raman spectrum [7] of oxyhcy all strongly suggest a binuclear, spin-coupled $[Cu^{II}-O_2^{-2}-Cu^{II}]$ bridging structure [8] for the oxygenated active site. In addition to O_2, the hemocyanins are also known to bind CO and NO.[9,10]

In spite of the information now available, copper(I) model compounds for the hcy–O_2 interaction have eluded chemists for more than 30 years, probably due largely to the paucity of information about Cu^{I} chemistry involving nitrogenous ligands in general and imidazole in particular.[11] In addition, the air sensitivity, kinetic lability, and tendency for disproportionation of Cu^{I} have exacerbated the problem.[12] The existence of copper(I) compounds exhibiting well defined reactivity with O_2 is poorly substantiated in the literature.[13–16] The first claim of a *reversible* Cu–O_2 interaction only recently appeared where an NOS_2 donor set was chosen as a reasonable model for the copper environment in hemocyanin.[17] However, only solid-state reactivity with O_2 was reported and the oxygenated product was identified only by e.s.r. spectroscopy with no information being given about the O_2 : Cu reaction stoicheiometry; furthermore, reactivity with O_2 in solution was reported to pro-

† Extended version of a plenary lecture read at the Fifth European Molecular Biology Organisation Meeting, Tours, August 1979; L. J. Wilson, C. L. Merrill, M. G. Simmons, J. M. Trantham, L. A. Bottomley, and K. M. Kadish, in 'Invertebrate Oxygen Binding Proteins. Structure, Active Site, and Function,' ed. J. Lamy, Marcel Dekker Inc., New York, 1980, in the press.

‡ For a recent review on synthetic Fe–O_2 carriers, see J. W. Buchler, *Angew. Chem. Internat. Edn.*, 1978, **17**, 407.

§ Extended *X*-ray absorption fine structure.

ceed irreversibly. Thus, to date there has been no authenticated example of a reversible Cu^{I} oxygen carrier in the solution state, despite the large number of synthetic O_2 complexes known for several other metals.*

The primary objective of this work was to design and synthesize discrete copper(I) complexes to serve as synthetic analogues for the hemocyanin active site and to explore the interaction of these species with O_2 and other small molecules. Our initial success has led to the novel five-co-ordinate {bis-2,6-[1-(2-imidazol-4-ylethylimino)-ethyl]pyridine}copper(I) cation {hereafter $[Cu^{I}(imep)]^{+}$} as shown in Figure 1(*a*). Preliminary results, reporting

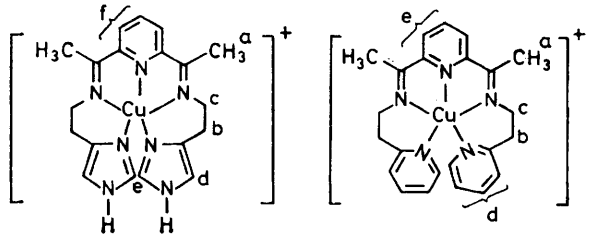

FIGURE 1 Structures for the $[Cu(imep)]^{+}$ (*a*) and $[Cu^{I}(pyep)]^{+}$ (*b*) cations. The H atom numbering is shown

the synthesis and characterization of the $[Cu^{I}(imep)]^{+}$ cation and establishing reversible binding of O_2 in solution, have been previously communicated,[18] and we now wish to report further results which include an extensive electrochemical examination of the deoxy and oxy form of $[Cu^{I,II}(imep)]^{n+}$. For completeness, the five-co-ordinate $[Cu^{II}(imep)]^{2+}$ and $[Zn^{II}(imep)]^{2+}$ species have also been prepared and characterized. Finally, the $[Cu^{I}(pyep)]^{+}$ complex in Figure 1(*b*) [along with the analogous copper(II) and zinc(II) compounds] is also reported here for comparative purposes because of our rather surprising finding that replacement of the imidazole moieties of Figure 1(*a*) by the terminal pyridine groups of Figure 1(*b*) results in loss of reversible O_2-binding capacity for the Cu^{I} centre. Thus, it was hoped that a detailed comparative examination of the $[Cu^{I}(imep)]^{+}$ and $[Cu^{I}(pyep)]^{+}$ cation properties would be enlightening as to the special requirements, if any, for Cu^{I} to function as an O_2-transport centre.

EXPERIMENTAL

Materials.—All solvents were reagent grade and were degassed by the standard freeze-thaw method. Acetonitrile was distilled from $K[MnO_4]$ and $Na_2[CO_3]$, and dimethyl sulphoxide (dmso) from BaO *in vacuo*. Histamine, free base (Grade B), was purchased from Calbiochem, and 2,6-diacetylpyridine and 2-(2-aminoethyl)-pyridine obtained from Aldrich Chemicals and used as received. Electrochemical grade tetrabutylammonium perchlorate (tbap) was purchased from G. Frederick Smith Chemical Co. or Eastman Chemicals and used without further purification. The compounds $Cu(ClO_4)_2 \cdot 6H_2O$ and $Zn(ClO_4)_2 \cdot 6H_2O$ were obtained from Alfa Products. Prepurified O_2 and CO for the manometric measurements were obtained from Matheson Gas Products.

Syntheses.—The Cu^{I} syntheses were performed under argon in a Vacuum/Atmospheres dry-box or using Schlenk glassware. Chemical analyses were obtained commercially.

Tetra(acetonitrile)copper(I) perchlorate, $[Cu^{I}(CH_3CN)_4][ClO_4]$. The compound was prepared by the method of Hemmerich and Sigwart.[19] Cu_2O (1.43 g) was added to a degassed solution of 0.2 mol dm^{-3} $HClO_4$ (100 cm^3) and CH_3CN (25 cm^3), then heated and stirred until the Cu_2O dissolved. Upon cooling, the white crystals which precipitate were collected by filtration and recrystallized from hot degassed CH_3CN. The purified product was collected and dried *in vacuo* at 80 °C for 12 h.

Tetra(acetonitrile)copper(I) tetrafluoroborate, $[Cu^{I}(CH_3CN)_4][BF_4]$. The compound was prepared by adding Cu_2O (1.43 g) to H_2O (106 cm^3) and CH_3CN (25 cm^3) and then adding dropwise $OEt_2 \cdot BF_3$ (3 cm^3). The solution was heated and stirred until the Cu_2O dissolved. Upon cooling, the white needles which precipitated were collected, recrystallized, and dried as above for the ClO_4^- salt.

{Bis-2,6-[1-(2-imidazol-4-ylethylimino)ethyl]pyridine}-copper(I) perchlorate, $[Cu^{I}(imep)][ClO_4]$. A ligand solution was prepared by dissolving 2,6-diacetylpyridine (1 mmol) and histamine (free base) (2 mmol) in degassed MeOH (25 cm^3). The mixture was stirred under reflux for 1 h to produce a light yellow solution. To this ligand solution, $[Cu^{I}(CH_3CN)_4][ClO_4]$ (1 mmol) dissolved in degassed CH_3CN (30 cm^3) was quickly added, giving an intense red-purple solution. The solution was reduced to dryness *in vacuo* and the resulting red solid was washed thoroughly with degassed H_2O and then with degassed CH_2Cl_2. The compound was recrystallized from hot degassed MeOH and dried *in vacuo* at 80 °C for 12 h. (Note: Some sample decomposition appeared to occur if P_2O_5 was used as a drying agent.) The copper(I) complex is obtained as very dark red, slightly hygroscopic platelets in 60% yield; $\Lambda_c = 177\ \Omega^{-1}\ dm^3\ mol^{-1}\ cm^{-1}$ for a 10^{-3} mol dm^{-3} CH_3CN solution at 30 °C; $\mu_{eff.}$(solid, 298 K) = 0.5 μ_B (Found: C, 44.15; H, 4.60; Cu, 12.25; N, 19.25. Calc. for $C_{19}H_{23}ClCuN_7O_4$: C, 44.55; H, 4.55; Cu, 12.4; N, 19.15%).

{Bis-2,6-[1-(2-imidazol-4-ylethylimino)ethyl]pyridine}copper(I) tetrafluoroborate–water (2/3), $[Cu^{I}(imep)][BF_4] \cdot 1.5H_2O$. The compound was prepared as for ClO_4^- salt, except that $[Cu^{I}(CH_3CN)_4][BF_4]$ was used as the source of Cu^{I}. The resulting dark red compound is considerably more hygroscopic than the ClO_4^- salt. Yield: 60%; $\Lambda_c = 150\ \Omega^{-1}\ dm^3\ mol^{-1}\ cm^{-1}$ for a 10^{-3} mol dm^{-3} CH_3CN solution at 30 °C; $\mu_{eff.}$(solid, 298 K) = 0.5 μ_B (Found: C, 43.5; H, 4.80; Cu, 12.1; N, 18.3. Calc. for $C_{19}H_{23}BCuF_4N_7 \cdot 1.5H_2O$: C, 43.3; H, 5.00; Cu, 12.05; N, 18.6%).

{Bis-2,6-[1-(imidazol-4-ylethylimino)ethyl]pyridine}copper(II) perchlorate, $[Cu^{II}(imep)][ClO_4]_2$. A ligand solution was prepared as for the above copper(I) complex. After the solution had cooled, $Cu(ClO_4)_2 \cdot 6H_2O$ (1 mmol) was added as a powdered solid which produced a dark green solution after

* In addition to the Fe–O_2 carriers in footnote ‡ (previous page), the following reviews cover the known O_2 carriers to date: R. G. Wilkins, in ' Bioinorganic Chemistry,' *Adv. Chem. Ser.*, 1971, **100**, 111; J. S. Valentine, *Chem. Rev.*, 1973, **73**, 235; F. Basolo, B. M. Hoffman, and J. A. Ibers, *Accounts Chem. Res.*, 1975, **8**, 384; G. McLendon and A. E. Martell, *Co-ordination Chem. Rev.*, 1976, **19**, 1; L. Vaska, *Accounts Chem. Res.*, 1976, **9**, 175; J. A. McGinnety, in ' MTP International Review of Science,' Series One, ed. D. W. A. Sharp, University Park Press, Baltimore, 1972, vol. 5; and R. D. Jones, D. A. Summerville, and F. Basolo, *Chem. Rev.*, 1979, **79**, 139.

several minutes of stirring. The solution was reduced to dryness *in vacuo* and the resulting green solid was washed thoroughly with H_2O and then with CH_2Cl_2. The compound was recrystallized from hot MeOH and the resulting dark green, slightly hygroscopic solid dried at 80 °C for 12 h. Yield: 70%; Λ_c = 346 Ω^{-1} dm^3 mol^{-1} cm^{-1} for a 10^{-3} mol dm^{-3} CH_3CN solution at 30 °C; $\mu_{eff.}$(solid, 298 K) = 1.8 μ_B (Found: C, 37.25; H, 3.80; Cu, 10.25; N, 16.85. Calc. for $C_{19}H_{23}Cl_2CuN_7O_8$: C, 37.3; H, 3.80; Cu, 10.4; N, 17.05%).

{*Bis*-2,6-[1-(2-*imidazol*-4-*ylethylimino*)*ethyl*]*pyridine*}*zinc*(II) *perchlorate*, $[Zn^{II}(imep)][ClO_4]_2$. The compound was prepared and treated identically to the above copper(II) compound. The light orange slightly hygroscopic solid was obtained in 70% yield; Λ_c = 350 Ω^{-1} dm^3 mol^{-1} cm^{-1} for a 10^{-3} mol dm^{-3} CH_3CN solution at 30 °C (Found: C, 37.0; H, 4.10; N, 15.75; Zn, 10.25. Calc. for $C_{19}H_{23}Cl_2N_7O_8Zn$: C, 37.2; H, 3.80; N, 16.0; Zn, 10.65%).

{*Bis*-2,6-[1-(2-*pyridin*-2-*ylethylimino*)*ethyl*]*pyridine*} *copper*(I) *perchlorate*, $[Cu^{I}(pyep)][ClO_4]$. A ligand solution was prepared by dissolving diacetylpyridine (1 mmol) in degassed MeOH (25 cm^3) and adding, dropwise, 2-(2-aminoethyl)-pyridine (2 mmol). This solution was stirred and gently heated for *ca.* 1 h, after which it appeared yellow in colour. $[Cu^{I}(CH_3CN)_4][ClO_4]$ (1 mmol) was then dissolved in degassed CH_3CN (30 cm^3) and added to the ligand solution. The resulting cherry-red solution was reduced to dryness *in vacuo*. The resulting brick-red solid was recrystallized from degassed CH_3CN–OEt_2 with cooling, collected by filtration, washed with OEt_2, and dried *in vacuo* at 80 °C for 12 h. Yield: 50%; Λ_c = 147 Ω^{-1} dm^3 mol^{-1} cm^{-1} for a 10^{-3} mol dm^{-3} CH_3CN solution at 30 °C; $\mu_{eff.}$(solid, 298 K) $\leq$0.2 μ_B (Found: C, 51.45; H, 4.75; Cu, 11.65; N, 13.2. Calc. for $C_{23}H_{25}ClCuN_5O_4$: C, 51.7; H, 4.70; Cu, 11.9; N, 13.1%).

{*Bis*-2,6-[1-(2-*pyridin*-2-*ylethylimino*)*ethyl*]*pyridine*} *copper*(II) *perchlorate*, $[Cu^{II}(pyep)][ClO_4]_2$. A ligand solution was prepared as for the above copper(I) complex. After the solution had cooled, $Cu(ClO_4)_2 \cdot 6H_2O$ (1 mmol) was added as a powdered solid. The blue solution which immediately resulted was filtered and reduced in volume to *ca.* 15 cm^3 and cooled to induce crystallization. The resulting blue-green crystals were dried *in vacuo* at 80 °C for 12 h. Yield: 50%; Λ_c = 339 Ω^{-1} dm^3 mol^{-1} cm^{-1} for a 10^{-3} mol dm^{-3} CH_3CN solution at 30 °C; $\mu_{eff.}$(solid, 298 K) = 2.1 μ_B (Found: C, 43.35; H, 3.90; Cu, 9.95; N, 10.95. Calc. for $C_{23}H_{25}Cl_2CuN_5O_8$: C, 43.55; H, 4.0; Cu, 10.0; N, 11.05%).

{*Bis*-2,6-[1-(2-*pyridin*-2-*ylethylimino*)*ethyl*]*pyridine*} *zinc*(II) *perchlorate*, $[Zn^{II}(pyep)][ClO_4]_2$. The compound was prepared in the same manner as described above for the copper(II) compound but using $Zn(ClO_4)_2 \cdot 6H_2O$. The pale yellow crystalline solid was obtained in 80% yield; Λ_c = 305 Ω^{-1} dm^3 mol^{-1} cm^{-1} for a 10^{-3} mol dm^{-3} CH_3CN solution at 30.0 °C (Found: 43.3; H, 3.80; N, 11.25; Zn, 10.7. Calc. for $C_{23}H_{25}ClN_5O_8Zn$: C, 43.45; H, 4.0; N, 11.0; Zn, 10.3%).

Electrochemistry.—Electrochemical measurements were obtained in CH_3CN, dmso, dimethylformamide (dmf), and pyridine solutions at room temperature under a constant flow of dry N_2 or Ar using a PAR model 174A polarographic Analyzer or a model 173 potentiostat/galvanostat driven by a model 175 universal programmer. The current voltage curves were recorded on a Houston Omnigraphic 2000 *X*—*Y* recorder at scan rates between 0.02 and 0.50 V s^{-1} and a Tektronix model 5111 storage oscilloscope at scan rates between 0.10 and 50 V s^{-1}. The electrolysis cell was a PAR polarographic model K60. A three-electrode geometry was employed, with a platinum button serving as the working electrode, a platinum wire as the counter electrode, and a Metrohm K901 saturated calomel electrode (s.c.e.) as the reference electrode. The reference electrode was separated from the bulk solution by means of a fritted-glass bridge containing supporting electrolyte solution. Solutions in the bridge were changed periodically to prevent aqueous contamination from entering the cell.

The overall number of electrons transferred was determined by controlled potential electrolysis in a standard H cell. Two platinum gauze electrodes of approximately equal surface area served as the cathode and the anode. The reference electrode (s.c.e.) was placed as close as possible to the cathode without shorting the circuit. Stirring of the solution was accomplished by bubbling N_2 through the solutions during electrolysis. Electronic integration of the current against time curve was achieved by means of a PAR model 179 coulometer and displayed as coulombs against time with the aid of a strip chart recorder. A Labchron digital timer was used to monitor all time measurements.

All solutions were 0.1 mol dm^{-3} in tetrabutylammonium perchlorate (tbap) and 10^{-3} mol dm^{-3} in complex. The maximum potential range in each solvent was checked by running a supporting electrolyte blank prior to each run. Dry N_2 and Ar were used interchangeably as degassing agents. The inert gas was presaturated with CH_3CN for measurements in that solvent to avoid evaporation. All potentials are reported against s.c.e. and are uncorrected for liquid junction potentials.

Physical and Spectroscopic Measurements.—Hydrogen-1 n.m.r. spectra were run at 90 MHz on a Varian EM390 spectrometer. Ultraviolet–visible spectra were obtained on a Cary 17 recording spectrophotometer. *X*-Band e.s.r. spectra were obtained at *ca.* 100 K on a Varian E-line spectrometer; field positions were referenced relative to dpph (diphenylpicrylhydrazyl) and detectable copper was quantitatively determined using $Cu[SO_4]$ samples of known concentrations for calibration. The oxy/deoxy cycled samples of $[Cu^{I}(imep)]^+$ shown in Figure 10 were obtained by extracting aliquots of the parent dmso solution and maintaining them as frozen glasses at liquid N_2 temperature until the spectra were recorded.

Magnetic susceptibilities of the solids were measured by the Faraday technique using a Cahn model 6600-1 research magnetic susceptibility system and $Hg[Co(NCS)_4]$ as the calibrant. All measurements were recorded at room temperature under 1 atm * He. Measured molar susceptibilities of the zinc(II) compounds were used to correct for ligand and anion diamagnetism: $[Zn^{II}(imep)][ClO_4]_2$: $\chi_M' = -2.980 \times 10^{-4}$ c.g.s. units mol^{-1}; $[Zn^{II}(pyep)][ClO_4]_2$: $\chi_M' = -1.702 \times 10^{-4}$ c.g.s. units mol^{-1}.

Oxygen uptake by $[Cu^{I}(imep)]^+$ in solution was measured at 23 °C by Warburg manometry. Flask constants were determined in the usual manner using triply distilled mercury as the calibrant.[20,21] Typically, a solid sample weighing *ca.* 20 mg was placed in the side arm of the manometer flask and *ca.* 3.0 cm^3 of degassed solvent in the bottom of the flask. After equilibration to constant temperature under flowing dry N_2, the manometer was flushed with prepurified O_2 for 1 min, adjusted to atmospheric pressure, closed to the atmosphere, and the solid dissolved by tilting the entire apparatus to mix the solid and solvent. An uptake measurement typically required 5—15 min for com-

* Throughout this paper: 1 atm = 101 325 Pa.

pletion. A solvent blank was treated in exactly the same manner as the sample solution and its uptake volume subtracted from the uptake volume of the sample. Solutions containing $[M^{II}(imep)]^{2+}$ or $[M^{II}(pyep)]^{2+}$ exhibited no O_2 uptake beyond that of pure solvent; the behaviour of the copper(I) compounds is discussed in the text below. The performance of the apparatus was checked using Vaska's iodide complex in benzene which forms an O_2 : Ir (1 : 1) adduct.[22] In general, O_2-uptake measurements were found to be reproducible within 10%.

RESULTS AND DISCUSSION

Synthesis and Characterization of the Complexes.—The synthetic scheme for $[Cu^{I}(imep)][ClO_4]$ is shown in Figure 2 where the imep ligand is generated by the Schiff-base condensation of free base histamine with

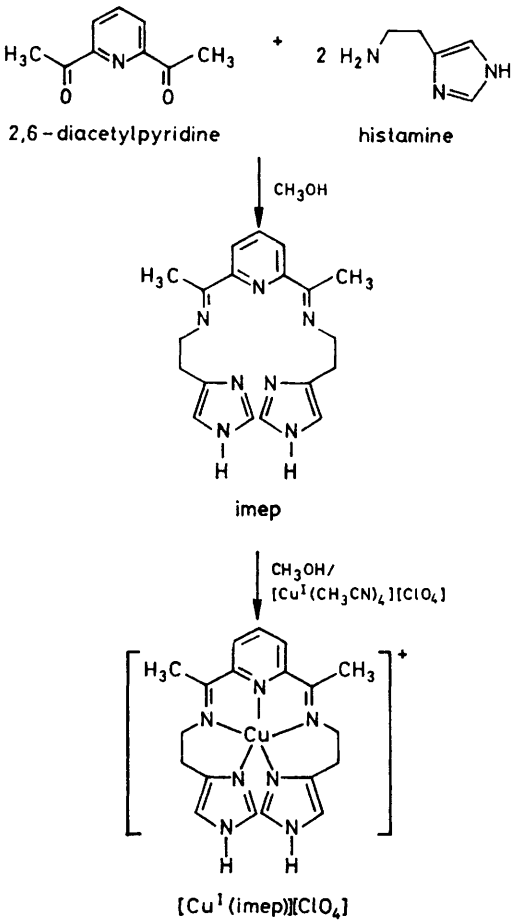

FIGURE 2 Synthetic scheme for the {bis-2,6-[1-(2-imidazol-4-ylethylimino)ethyl]pyridine}copper(I) perchlorate complex

2,6-diacetylpyridine. Addition of $[Cu^{I}(CH_3CN)_4][ClO_4]$ under Ar results in an intense red solution from which $[Cu^{I}(imep)][ClO_4]$ is isolated as a dark red solid. Thus, the copper(I) complex can be conveniently prepared by direct reaction of a multidentate ligand with a copper(I) salt without resorting to electrochemical preparative methods which are sometimes necessary to avoid disproportionation.[12] Substitution of $Cu(ClO_4)_2 \cdot 6H_2O$ or $Zn(ClO_4)_2 \cdot 6H_2O$ in the synthesis yields the dark green copper(II) salt or the light orange Zn^{II} species, respectively. If 2-(2-aminoethyl)pyridine is substituted for histamine in the synthesis, addition of $[Cu^{I}(CH_3CN)_4][ClO_4]$ under Ar produces a red solution from which $[Cu^{I}(pyep)][ClO_4]$ is isolated as a brick-red solid; analogously, the yellow zinc(II) and blue-green copper(II) complexes can also be directly synthesized by this procedure using the appropriate metal salt. As indicated above in Figure 1, the imep and pyep ligands are assumed to function in a fully quinquedentate fashion for all the complexes of Cu^{I}, Cu^{II}, and Zn^{II} reported here. This fact has recently been verified in the solid state by structural determinations of $[M(imep)][ClO_4]_2$ ($M = Cu^{II}$ or Zn^{II}) where the nitrogen-donor atom co-ordination spheres about the metal ions are best described as arrayed in a very distorted square pyramid.* For the copper(I) compounds, such definitive structural information is presently lacking; † however, five-co-ordinate Cu^{I} is not unknown [12] and available analytical, solution conductivity data (Experimental section), and ^1H n.m.r. spectra are not inconsistent with five-co-ordinate formulation.

The ^1H n.m.r. spectra of the $[Zn^{II}(imep)]^{2+}$, $[Zn^{II}(pyep)]^{2+}$, and $[Cu^{I}(pyep)]^{+}$ cations in CD_3CN are given in Figure 3, along with the proton resonance assignments as shown in Figure 1. The actual signal positions are reported in Table 1. Spectra for all three of the compounds are consistent with the formulation of the complexes as five-co-ordinate species in solution since there appears to be no additional multiplicity of the kind possible for unco-ordinated ligand arms. A spectrum of $[Cu^{I}(imep)]^{+}$ has been obtained only as an extremely broadened version of its Zn^{II} analogue in Figure 3(*a*). In this instance, the observed severe spectral broadening is most reasonably attributed to the presence of trace paramagnetic Cu^{II} ' contaminants ' which are produced

TABLE 1

Hydrogen-1 n.m.r. signal positions and assignments for the copper(I) and zinc(II) compounds in CD_3CN at room temperature

Compound	Proton assignment [a]	Shift (p.p.m.) [b]
$[Zn^{II}(imep)]^{2+}$	a	2.54
	b	3.18
	c	3.97
	d	7.20
	e	8.00
	f	8.37
$[Zn^{II}(pyep)]^{2+}$	a	2.57
	b	3.45
	c	4.19
	d	7.62—8.08
	e	8.46
$[Cu^{I}(pyep)]^{+}$	a	2.27
	b	3.56
	c	4.13
	d, e	7.0—8.5

[a] Refers to Figure 1. [b] Referenced to internal $SiMe_4$.

* J. D. Korp, I. Bernal, and L. J. Wilson, unpublished work. The five-co-ordinate $[M(imep)][ClO_4]_2$ ($M = Zn^{II}$ or Cu^{II}) compounds are isomorphous and isostructural. For example, the M–N bond distances for the zinc(II) compound are: $Zn-N_{(py)}$, $Zn-N_{(imine)} = 2.00$ Å and $Zn-N_{(imidazole)} = 2.19$ Å.

† The structure of $[Cu^{I}(pyep)][BF_4]$ is in progress.

because of the extremely O_2-sensitive nature of the $[Cu^{I}(imep)]^{+}$ cation in solution (see below).

In solution, the green $[Cu^{II}(imep)]^{2+}$ complex exhibits *d–d* absorption bands centred at *ca.* 750 nm with $\varepsilon_{max.}$ (670 nm) = 136 dm^3 mol^{-1} cm^{-1} for the higher energy component, as shown in Figure 4(*a*). Furthermore, the shape and position of the absorption envelope is essentially solvent independent for CH_3CN, dmf, dmso, pyridine, and 2,6-lutidine. Since the absorption spectrum closely resembles that of other established five-co-ordinate Cu^{II} species,[23-25] it is inferred that the $[Cu^{II}(imep)]^{2+}$ cation maintains its integrity in solution and remains five-co-ordinate even in strongly ligating solvents. This view is further supported by the solid-state spectrum (as a Nujol mull) which appears identical to the solution-state spectra. In contrast, the absorption spectrum for $[Cu^{II}(pyep)]^{2+}$ is more solvent dependent, as shown in Figure 4(*b*), although spectra obtained in CH_3CN, dmso, and dmf are indistinguishable and, therefore, consistent with the preservation of a five-co-ordinate Cu^{II} centre in these solvent systems. As a point of interest, for copper(II) hemocyanin, a *d–d* band is also present but at a higher energy (570 nm) and greater intensity (ε = 500 dm^3 mol^{-1} cm^{-1}).[26]

The copper(I) complexes exhibit an electronic absorption spectrum in the visible region which accounts for their intense red colours. For the $[Cu^{I}(pyep)]^{+}$ cation, the spectrum as recorded in various degassed solvents is shown in Figure 5. As can be seen from the Figure, the spectrum is somewhat solvent dependent in that the moderately intense charge-transfer (c.t.) band [$\varepsilon_{max.}$ (500 nm) $\geqslant$ 2 000 dm^3 mol^{-1} cm^{-1}] varies with respect to intensity and, in one case, multiplicity in dmso. The analogous $[Cu^{II}(pyep)]^{2+}$ species is devoid of any such c.t. band in the visible; and in pyridine solution, the band is also absent for $[Cu^{I}(pyep)]^{+}$ which is assumed to result from either compound decomposition or pyridine ligation in that solvent. Thus, both the Cu^{I} and Cu^{II} $[M(pyep)]^{n+}$ cations show spectral indication of solvent

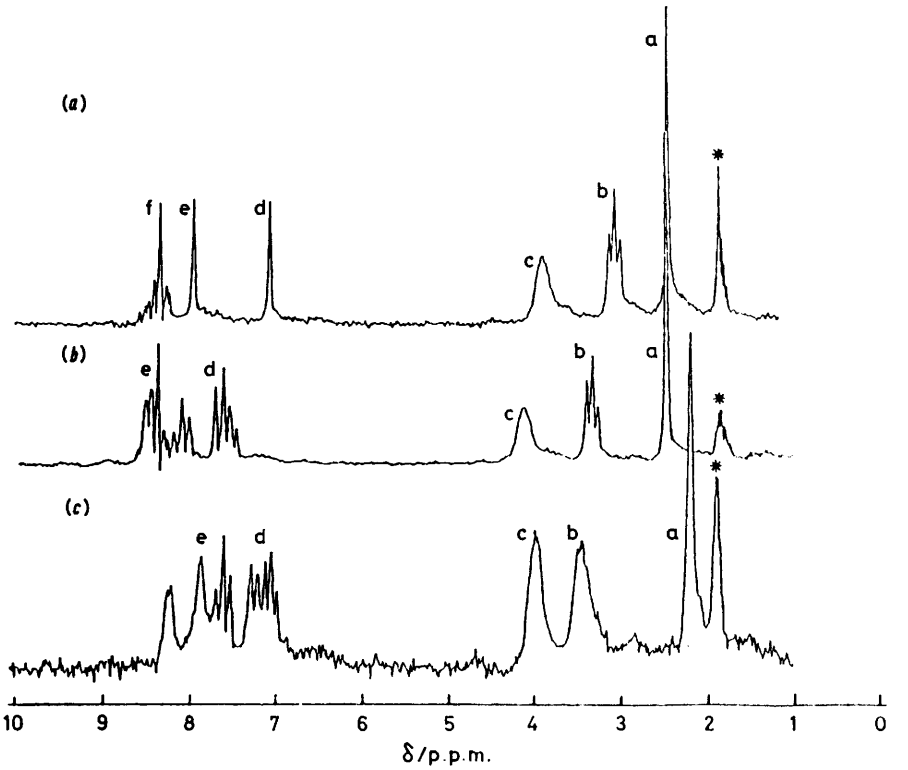

FIGURE 3 Proton magnetic resonance spectrum of (*a*) $[Zn^{II}(imep)]^{2+}$, (*b*) $[Zn^{II}(pyep)]^{2+}$, (*c*) $[Cu^{I}(pyep)]^{+}$; in CD_3CN at room temperature with signals referenced to internal $SiMe_4$. Asterisks refer to solvent resonances. Indicated proton assignments are shown in Figure 1

'involvement' in their solution chemistries. In contrast, however, the $[Cu^{I}(imep)]^{+}$ complex exhibits an electronic spectrum in degassed solvents in which the position and multiplicity of the c.t. band ($\lambda_{max.}$ *ca.* 520 nm) is essentially independent of solvent for dmso, CH_3CN, dmf, and pyridine. A typical spectrum as taken in degassed dmso is shown in Figure 6(*a*). Thus, as for its Cu^{II} analogue, the $[Cu^{I}(imep)]^{+}$ cation appears to remain five-co-ordinate even in potentially ligating solvents.

Reactivity of $[Cu^{I}(imep)]^{+}$ *with Oxygen in Solution.*—The most striking property exhibited by solutions of $[Cu^{I}(imep)]^{+}$ is the change in colour from red to green upon exposure to O_2 and the reverse colour change when the solution is degassed under reduced pressure. The

accompanying spectral changes in the visible region for three oxy/deoxy cycles are shown in Figure 6. In degassed dmso, dmf, or pyridine, the $[Cu^{I}(imep)]^{+}$ complex exhibits a c.t. band centred at 520 nm with $\varepsilon_{max.}$ *ca.* 1 400 $dm^3\ mol^{-1}\ cm^{-1}$ as shown in Figure 6(*a*) for dmso. If this red solution is exposed to prepurified O_2 (1 atm; room temperature) for *ca.* 5 min, O_2 is absorbed and a light green coloured solution is produced, giving spectrum 6(*b*). Manometric measurements by Warburg manometry (see Experimental section) have verified the O_2 uptake in solution to be stoicheiometric and reproducible from sample to sample with oxygenation proceeding

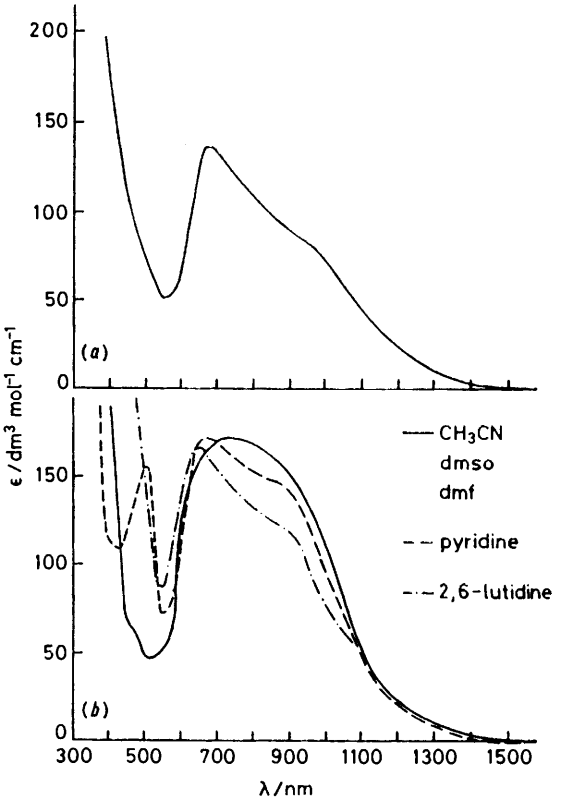

FIGURE 4 Electronic absorption spectra in the visible region for the copper(II) complexes at 2×10^{-3} mol dm^{-3}: (*a*) $[Cu^{II}(imep)]^{2+}$ in dmso, dmf, CH_3CN, pyridine, and 2,6-lutidine (showing the solvent independency); (*b*) $[Cu^{II}(pyep)]^{2+}$ in various solvents

rapidly (5—15 min) until 0.5 mol (±10%) of O_2 is absorbed per available copper, after which uptake decreases to a trace level. Typical manometric results in dmso are documented in Table 2. Thus, the manometric results firmly establish the O_2 : Cu stoicheiometry as 1 : 2 for the first oxy cycle, indicating formation of a μ-dioxygen bridged copper species similar to the situation proposed to exist for oxyhemocyanin.

A freshly oxygenated $[Cu^{I}(imep)]^{+}$ solution can then be deoxygenated under reduced pressure for *ca.* 20 min to produce the original red coloured solution and the electronic spectrum shown in Figure 6(*c*). Similar spectral and manometric results are also obtained for dmf or pyridine solutions of $[Cu^{I}(imep)]^{+}$, although quali-

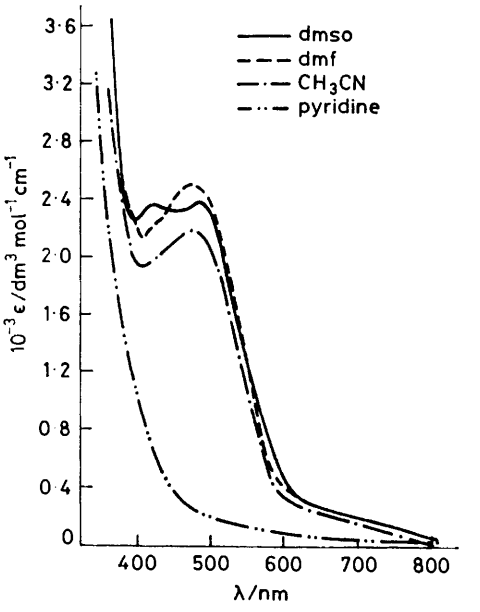

FIGURE 5 Electronic absorption spectrum in the visible region of $[Cu^{I}(pyep)]^{+}$ at 5×10^{-4} mol dm^{-3} in various degassed solvents

tatively, the rate of O_2 uptake (1 atm O_2; room temperature) is solvent dependent according to the ordering: dmf (1—2 min) < dmso (*ca.* 5 min) < pyridine (*ca.* 15 min). The BF_4^- salt behaves similarly but the oxygenation rates are perceptibly slower than for ClO_4^-. Once deoxygenated, any of the solutions will reabsorb O_2 and

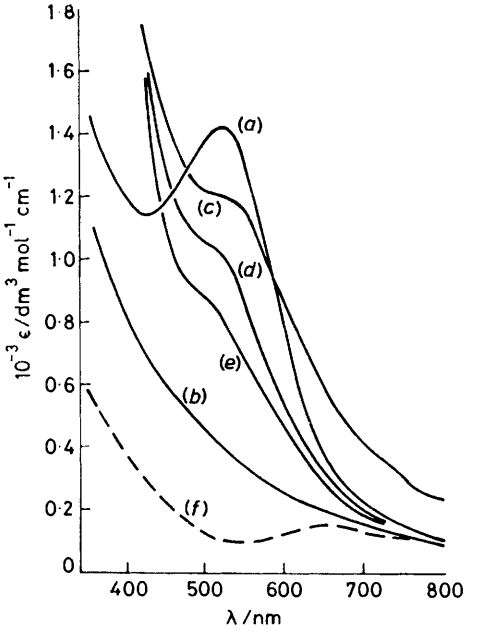

FIGURE 6 Electronic absorption spectrum in the visible region of (*a*) $[Cu^{I}(imep)]^{+}$ in degassed dmso at 5×10^{-4} mol dm^{-3}; (*b*) solution (*a*) after oxygenation under 1 atm for 5 min with absorption of 0.5 moles of O_2 per Cu; (*c*) solution (*b*) after deoxygenation under reduced pressure; (*d*) solution (*b*) after a second oxy/deoxy cycle; (*e*) solution (*b*) after a third oxy/deoxy cycle; (*f*) $[Cu^{II}(imep)]^{2+}$ in dmso at 5×10^{-3} mol dm^{-3} (showing spectral transparence at 520 nm)

again turn green during a second oxy/deoxy cycle, but with the O_2 uptake being only *ca.* 80% of the initial uptake volume. Figure 6(*d*) displays the spectrum of the red, deoxy $[Cu^{I}(imep)]^{+}$ solution after a second oxy/deoxy cycling, and 6(*e*) the spectrum after a third cycle. Thus, taken together, the manometric and spectral data of Figure 6 are in good agreement in establishing a *ca.* 80% reversibility factor of O_2 binding in solution under ambient conditions for the $[Cu^{I}(imep)]^{+}$ cation. Low-temperature measurements, to be reported later in conjunction with thermodynamic studies of O_2 binding,[27]

TABLE 2

Manometric O_2-uptake data for $[Cu^{I}(imep)][ClO_4]$ in dmso at 23 °C [a]

Expt. no.	Moles Cu ($\times 10^{-6}$)	Moles O_2 ($\times 10^{-6}$) [b]	O_2 : Cu Ratio [c]
1	11.01	4.92	0.48 : 1
2	5.66	2.64	0.47 : 1
3	5.85	3.04	0.52 : 1
4	4.88	2.50	0.51 : 1

[a] Determined by Warburg manometry as described in the Experimental section. [b] A typical uptake measurement proceeded rapidly, requiring 5—15 min, after which O_2 absorption decreased to a trace level. [c] As indicated, O_2-uptake measurements by the Warburg method were found to be typically reproducible within 10% and thus consistent with a O_2 : Cu stoicheiometry of 1 : 2 for the 90—95% purity level of the copper(I) compound (see below: e.s.r. section).

indicate improvement beyond the 80% reversibility level at lower temperatures. Finally, after multiple oxy/deoxy cycles at room temperature, oxygenated solutions cannot be reconverted to the original red form, and a similar result occurs if freshly prepared solutions are oxygenated and ' aged ' for 1 h or so at room temperature. Furthermore, it is interesting to note that the $[Cu^{I}(imep)]^{+}$ complex exhibits no discernible reactivity with CO as monitored manometrically and electrochemically (see below) and that the compound decomposes rapidly in the presence of NO. Thus, in this regard, $[Cu^{I}(imep)]^{+}$ fails to mimic the hemocyanins which are known to bind both CO and NO.[8,9] Of course, solutions of $[Cu^{II}(imep)]^{2+}$ and $[Zn(imep)]^{2+}$ show no tendency to react with O_2 or CO, and again NO only promotes compound decomposition.

Of the $[M(pyep)]^{n+}$ compounds, only the Cu^{I} species displays reactivity with O_2 (but not with CO). However, unlike the $[Cu^{I}(imep)]^{+}$ species, the complex does not react appreciably within *ca.* 15 min exposure, although over longer periods of time (h) a very slow and apparently continuous uptake of O_2 is observed, as is indeed also the case for the $[Cu^{I}(imep)]^{+}$ compound. This long term O_2 reaction is irreversible and the final products have not been identified. Thus, of the two copper(I) complexes, only the imidazole-bearing $[Cu^{I}(imep)]^{+}$ species appears to function as a legitimate oxygen carrier that can be reversibly cycled; however, both copper(I) complexes also display a much slower and longer term irreversible reaction with O_2 which is likely to involve ligand oxidation or perhaps even a catalytic reaction of some nature.[28,29] For example, one such reaction has recently been reported where ligand hydroxylation occurs.[30] To date, however, all attempts (including low-temperature reaction conditions) have failed to yield well characterized oxygenated $[Cu^{I}(imep)]^{+}$ derivatives or compounds of the longer term oxygenation/oxidation reaction. As solids, both of the copper(I) compounds appear stable toward dry O_2, although as a precaution they have been handled routinely under an inert atmosphere.

Electrochemical Studies.—Cyclic voltammograms were obtained for both copper(II) complexes in the presence and absence of dissolved O_2. Half-wave potential measurements were made in CH_3CN, dmf, dmso, and pyridine. In the absence of O_2, $[Cu^{II}(imep)]^{2+}$ and $[Cu^{II}(pyep)]^{2+}$ are both characterized by reversible, one-electron redox processes. Current functions and half-wave potentials were independent of scan rate over the range 0.02 to 10 V s^{-1} indicating a diffusion-controlled electron transfer.[31] In addition, separations between the anodic and cathodic peak potentials were consistent with a one-electron oxidation–reduction process in each solvent examined. Formation of the red Cu^{I} species, by addition of one electron to the green copper(II) complex, was verified by controlled-potential electrolysis at potentials 250 mV cathodic of $E_{\frac{1}{2}}$. Reversibility of this process was confirmed by subsequent controlled-potential oxidation giving quantitative yields. The reversible half-wave potentials for each $Cu^{II} \rightleftharpoons Cu^{I}$ process are compiled in Table 3.

A typical cyclic voltammogram for reduction of $[Cu^{II}(pyep)]^{2+}$ and oxidation of $[Cu^{I}(pyep)]^{+}$ is shown in Figure 7. Identical half-wave potentials were obtained for both complexes. As seen from Table 3, potentials

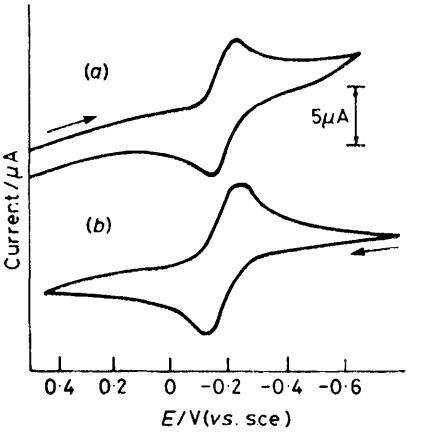

FIGURE 7 Cyclic voltammograms for the copper complexes in degassed CH_3CN at 10^{-3} mol dm^{-3} and 0.1 mol dm^{-3} tbap. Scan rate = 200 mV s^{-1}: (*a*) $[Cu^{II}(pyep)]^{2+}$; (*b*) $[Cu^{I}(pyep)]^{+}$

for $[Cu^{II}(pyep)]^{2+}$ reduction are *ca.* 130 mV more positive than for reduction of $[Cu^{II}(imep)]^{2+}$. This difference in potential is independent of solvent and indicates a greater stability of the Cu^{I} oxidation state in the pyridine-ligated complex. This result is reasonable since pyridine is known to be a superior π-back-bonding ligand when compared to imidazole [32-34] and thus should have a greater capacity for stabilizing Cu^{I}.

Table 4 summarizes the electrochemical data obtained in CH_3CN for all the complexes of Cu^I, Cu^{II}, and Zn^{II}. In CH_3CN, $[Zn^{II}(pyep)]^{2+}$ gives a reversible, one-electron reduction at −1.08 V which probably corresponds to a ligand centred reduction yielding the anion radical. At scan rates of less than 2 V s^{-1} the reduced $[Zn^{II}(imep)]^{2+}$ complex does not yield an anodic wave. However, the

TABLE 3

Cyclic voltammetric data for the copper complexes at 10^{-3} mol dm^{-3} and 0.1 mol dm^{-3} in tbap

Compound	Solvent	$E_{\frac{1}{2}}(Cu^{II} \rightleftharpoons Cu^{I})$ (V *vs.* s.c.e.)
$[Cu^{II}(imep)]^{2+}$	CH_3CN	−0.30
	dmf	−0.27
	dmso	−0.27
	Pyridine	−0.20
$[Cu^{II}(pyep)]^{2+}$	CH_3CN	−0.17
	dmf	−0.13
	dmso	−0.15
	Pyridine	Irreversible

cathodic peak current was proportional to $v^{\frac{1}{2}}$ at high scan rates and $|E_p - E_{\frac{p}{2}}| = 60 \pm 10$ mV, suggesting a reversible one-electron transfer followed by a rapid chemical reaction (e.c. mechanism).[31] As predicted, cathodic peak potentials shifted by 30 mV (log $v)^{-1}$ at slower scan rates. Reversible peaks were obtained at scan rates >10 V s^{-1}. No attempt has been made to identify the reduction products of either zinc(II) complex. It is tempting to rationalize the existence of this e.c. process for the $[Zn^{II}(imep)]^{2+}$ complex as due to the presence of the imidazole proton which is involved in the reaction of the anion radical following electron transfer.

Cyclic voltammetry may provide a convenient method of observing the oxygenation process for $[Cu^{I}(imep)]^{+}$, as it is generated at the electrode surface from its Cu^{II} analogue. Figure 8 shows the cyclic voltammogram of $[Cu^{II}(imep)]^{2+}$ in the presence and absence of dissolved O_2 in dmso. At a scan rate of 200 mV s^{-1}, identical voltammograms were obtained indicating no effect of O_2 within the time scale of the experiment. However, if the potential was held at −0.60 V for 9 s [Figure 8(*c*)],

TABLE 4

Cyclic voltammetric data for the ClO_4^- salts in degassed CH_3CN at 10^{-3} mol dm^{-3} and 0.1 mol dm^{-3} in tbap

Compound	$E_{\frac{1}{2}}$ (V *vs.* s.c.e.)	$\lvert E_p - E_{\frac{p}{2}}\rvert$ [a] (V)
$[Cu^{II}(imep)]^{2+}$	−0.30	0.072
$[Cu^{II}(pyep)]^{2+}$	−0.17	0.060
$[Cu^{I}(pyep)]^{+}$	−0.17	0.060
$[Zn^{II}(imep)]^{2+}$	−1.17	0.050 [b]
$[Zn^{II}(pyep)]^{2+}$	−1.08	0.060

[a] Measured at a scan rate of 0.10 V s^{-1} unless otherwise indicated. [b] Measured at a scan rate of 10 V s^{-1}.

oxidation of the reduction product was not observed, indicating that the Cu^I species generated at the electrode surface had undergone a chemical reaction. The potential sweep was reversed at −0.60 V in order not to reduce any dissolved O_2 to O_2^-.[35] When the potential was held at −0.60 V for the same complex under N_2, a completely reversible wave was obtained, thus demonstrating that the observed behaviour is indeed due to reaction of electrochemically generated $[Cu^{I}(imep)]^{+}$ with O_2. Furthermore, if an O_2-saturated solution, that has once given a voltammogram like that in Figure 8(*c*), is thoroughly degassed with N_2, the reversible anodic wave is totally recovered, further establishing the reversible nature of the oxygenation reaction in solution. This electrochemically observed reaction of $[Cu^{I}(imep)]^{+}$ with O_2, which occurs in seconds after the copper(I) compound is generated at the electrode surface, is not necessarily inconsistent with the much slower (5—15 min) O_2-uptake rate of the Warburg measurement; in the latter case.

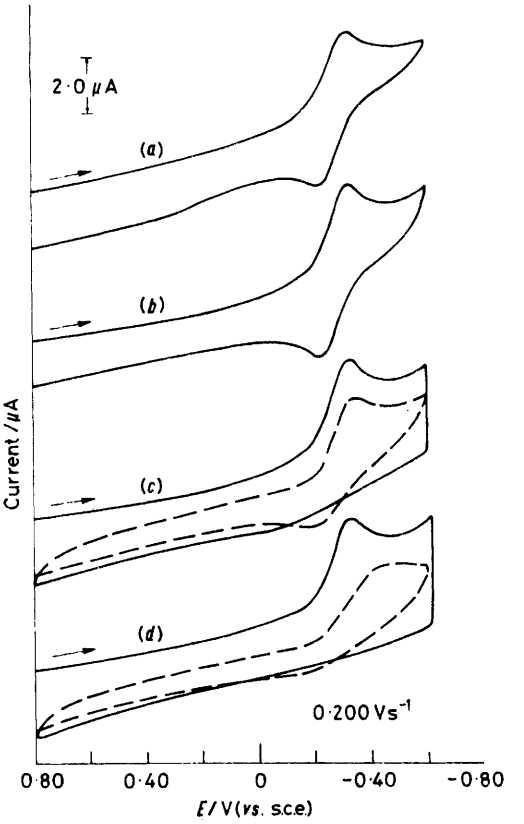

FIGURE 8 Cyclic voltammograms of 1.6 mmol dm^{-3} $[Cu^{II}(imep)]^{2+}$ in dmso 0.1 mol dm^{-3} in tbap. Scan rate = 200 mV s^{-1}. (*a*) Under N_2; (*b*) under O_2; (*c*) under O_2, where the potential was held after the first cathodic sweep at −0.60 V for 9 s, then scanned anodically (——), and cycled with no hold in potential for second scan (– – – –); (*d*) same conditions as (*c*) but with a hold in potential for 27 s at −0.60 V

oxygenation is likely rate determined by diffusion of O_2 into solution, whereas the electrochemistry is performed on solutions already saturated with O_2 and in the presence of a potentially catalytic platinum electrode surface. The second sweep, shown in Figure 8(*c*), reveals a regeneration of $[Cu^{II}(imep)]^{2+}$ and its normal coupled oxidation. When the potential was held at −0.60 V for 27 s, as in Figure 8(*d*), no anodic process was observed on the reverse sweep. With a longer time delay, the second cathodic scan again showed the apparent regeneration of $[Cu^{II}(imep)]^{2+}$. However, there was a 100-mV shift in the second reduction potential concomitant with a de-

crease in peak current and a broadening of peak shape. This behaviour at longer exposure times to O_2 is consistent with a slow chemical reaction preceding the electron transfer to yield Cu^I (a c.e. mechanism).[31]

Based on electrochemical results and the known chemistry of the oxygenated species, the mechanism shown in Figure 9 is proposed for the electroreduction of $[Cu^{II}(imep)]^{2+}$ in the presence of O_2. The initial electron-transfer reaction at −0.20 to −0.30 V (depending on solvent) is followed by a reversible addition of O_2 to the product to yield a monomeric Cu^I–O_2 complex. At short

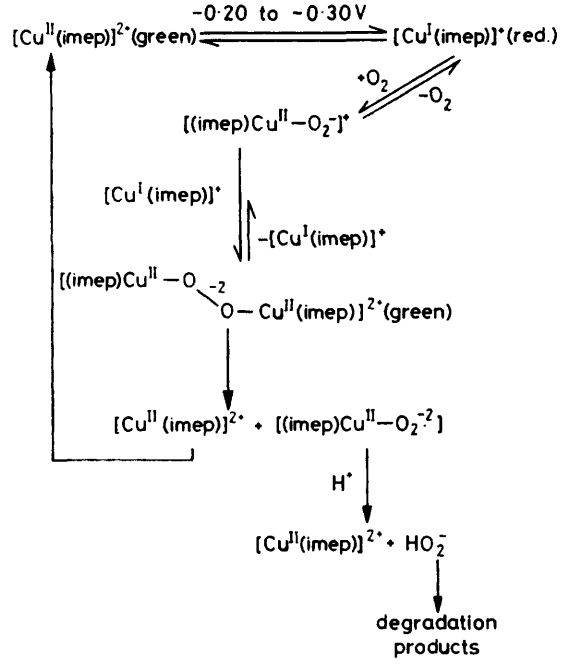

FIGURE 9 Proposed electrode mechanism for the reduction of $[Cu^{II}(imep)]^{2+}$ in the presence of O_2

time delays (*i.e.* <9 s), this species may dissociate to yield $[Cu^I(imep)]^+$ which is oxidized to the copper(II) complex, or at the longer delay times, which will react with a second unoxygenated $[Cu^I(imep)]^+$ molecule to form a binuclear Cu^{II} peroxo-species, $[(imep)Cu^{II}–O_2^{-2}–Cu^{II}(imep)]^{2+}$. This reaction intermediate can then dissociate to yield the original copper(II) complex, $[Cu^{II}(imep)]^{2+}$, and accounts for the c.e. mechanism observed in Figure 8(*d*). The proposed $[(imep)Cu^{II}–O_2^{2-}]$ species also formed on splitting the dimer might then further react to yield reactive species such as O_2^{2-} or HO_2^- which would likely degrade the copper complexes in solution.

It is now generally accepted, largely on the basis of Co^{II}–O_2 work, that O_2 adds to the metal centre *via* an internal oxidative addition reaction, in which the metal is

$$M^{n+} + O_2 \rightarrow [M^{(n+1)+} - O_2^-]$$

oxidized and the O_2 reduced.[36] If this formalism is adopted here, then an electron transfer from Cu^I is surely concomitant with O_2 adduct formation, so that the species to be oxidized on the reverse anodic scan formally contains Cu^{II}, and thus, no oxidation wave is to be expected. The initial product of oxygenation is likely monomeric, *i.e.* $[(imep)Cu^{II}–O_2^-]$, as a first step in the ultimate formation of the binuclear species, $[(imep)Cu^{II}–O_2^{-2}–Cu^{II}(imep)]$. (Resonance Raman studies are in progress to test the appropriateness of viewing the μ-dioxygen centre as μ-peroxo.) All oxygenated solutions eventually decompose within a few hours, changing colour and sometimes producing brown precipitates. Thus, Figure 9 would seem to summarize events consistent with the observed behaviour for the overall oxygenation process as initiated by the electrochemical generation of $[Cu^I(imep)]^+$.

The $[Cu^I(imep)]^+$ complex exhibits the same oxygenation behaviour in dmso, CH_3CN, dmf, and pyridine, but the rate is clearly solvent dependent as noted above: $CH_3CN \simeq$ dmf > dmso > pyridine. In CH_3CN, for example, even a fast (200 mV s^{-1}) scan in O_2-saturated solutions did not yield an anodic peak. This cyclic voltammetry result corroborates the above qualitative observations that there is a substantial solvent effect on the oxygenation rate. Since the electrochemical measurements occur in saturated O_2 solutions, it is inferred that the observed rate dependence is not due to bulk solvent properties such as rate of O_2 dissolution, but rather to [solvent • • • $Cu^I(imep)^+$] interactions of some nature. Since the observed rates parallel solvent characteristics such as donor number[37] and basicity,[38] the correlations suggest some solvent promoted inhibition to the site of O_2 co-ordination at Cu^I. However, since the above electronic spectral data for $[Cu^I(imep)]^+$ give no indication of solvent participation in the primary co-ordination sphere, it may be that solvent molecule association with the ligand periphery affects the oxygenation rate. The common characteristic of the solvents used in this study is their basicity, and thus an acidic ligand site seems most likely for such a solvent interaction. The most acidic proton of the molecule is, of course, the imidazole proton which would be most susceptible to solvent interactions such as hydrogen bonding.

In contrast to the $[Cu^I(imep)]^+$ species, the electrochemically generated Cu^I reduction product of $[Cu^{II}(pyep)]^{2+}$ does not show any reactivity with O_2 using the same conditions given in Figure 8 (or for even longer hold times of up to several minutes). Similarly, CO-saturated solutions of $[Cu^{II}(imep)]^{2+}$ and $[Cu^{II}(pyep)]^{2+}$ in dmso give cyclic voltammograms essentially identical in appearance, under all of the above conditions, to those obtained under only N_2. Thus, the electrochemical, as well as the above manometric results, are in agreement in indicating a reversible oxygenation reaction for only $[Cu^I(imep)]^+$ in solution and no reaction at all for $[Cu^I(imep)]^+$ or $[Cu^I(pyep)]^+$ with CO under ambient conditions.

Electron Spin Resonance Spectra.—Consistent with the O_2-uptake stoicheiometry, the final product of the reversible oxygenation of $[Cu^I(imep)]^+$ is probably the binuclear species, $[(imep)Cu^{II}–O_2^{-2}–Cu^{II}(imep)]$. It

is possible that such an oxygenated adduct would be diamagnetic *via* antiferromagnetic exchange between formally Cu^{II} ($S = \frac{1}{2}$) centres, as is thought to be the case for oxyhemocyanin which is also e.s.r. silent.[5,39] However, unlike the present synthetic Cu_2O_2 unit, oxyhemocyanin may also contain an additional endogenous bridge.[40] In Figure 10, the e.s.r. spectra of $[Cu^{II}(imep)]^{2+}$ (*a*) and $[Cu^{I}(imep)]^{+}$ (*b*) are shown as dmso glasses at *ca.* 100 K. Both spectra have the characteristic signature of magnetically dilute Cu^{II} with normal $g_{\|}$, $A_{\|}$, and $g_{\perp}$ values, but with only 5—10% of available copper in the $[Cu^{I}(imep)]^{+}$ sample being detected as paramagnetic Cu^{II}. Thus, a small amount of some Cu^{II} ' contaminant ' is apparently produced during the synthesis and handling of the $[Cu^{I}(imep)]^{+}$ sample, and to date, we have been unable to reduce its presence much below the 5% level. It should be noted that at this level, and with a composition close to $[Cu^{II}(imep)]^{2+}$, this Cu^{II} ' contaminant ' would not be expected to adversely affect the chemical analysis of the copper(I) compound nor to invalidate the O_2-uptake measurements which are accurate to only $\pm 10\%$. However, its presence is likely to be responsible for the lack of a resolved ^1H n.m.r. spectrum for the copper(I) complexes and for the slightly higher magnetic moment of the $[Cu^{I}(imep)]X$ compounds ($\mu_{eff.} = 0.5\ \mu_B$) as compared to that for the relatively O_2-insensitive $[Cu^{I}(pyep)][ClO_4]$ compound ($\mu_{eff.} \leqslant 0.2\ \mu_B$). Consistent

TABLE 5

E.s.r. data for the copper complexes as dmso glasses at *ca.* 100 K, [Cu] = 10^{-3} mol dm^{-3}

Compound	$g_{\|}$	$10^3 A_{\|}/cm^{-1}$ (A in G)	$g_{\perp}$
$[Cu^{II}(imep)]^{2+}$	2.27	18.0 (170)	2.06
$[Cu^{II}(pyep)]^{2+}$	2.21	15.5 (150)	2.05
$[Cu^{I}(imep)]^{+}$ *			
(*b*)	2.22	15.0 (145)	2.10
(*c*)	2.23	14.6 (140)	2.10
(*d*)	2.22	15.5 (150)	2.09
(*e*)	2.22	15.5 (150)	2.09
(*f*)	2.22	15.0 (145)	2.09

* Refers to Figure 10; only 5—10% of available copper is detected as Cu^{II}.

with this interpretation, the $[Cu^{I}(pyep)]^{+}$ cation gives a normal ^1H n.m.r. spectrum (Figure 3), but no e.s.r. spectrum when compared to the integrated intensity of its $[Cu^{II}(pyep)]^{2+}$ analogue at 10^{-3} mol dm^{-3} in dmso. The $g_{\|}$, $A_{\|}$, and $g_{\perp}$ spectral parameters for all the e.s.r. active samples are summarized in Table 5 for comparison purposes.

Also shown in Figure 10 (*b*)—(*f*) and in Table 5 are e.s.r. spectral data obtained during various stages of oxy/deoxy cycling of $[Cu^{I}(imep)]^{+}$. Spectrum (*c*) recorded after the first oxygenation step with $O_2 : Cu = 0.5 : 1$, is remarkably similar to (*b*) with no perceptible increase in signal intensity or multiplicity upon oxygenation. Thus, the present $[Cu^{II}–O_2^{-2}–Cu^{II}]$ binuclear unit appears to electronically mimic the e.s.r. silent behaviour of oxyhemocyanin where the Cu^{II} centres are fully spin-coupled with $-J \geqslant 550\ cm^{-1}$.[39] Full temperature-susceptibility measurements on oxygenated solutions of $[Cu^{I}(imep)]^{+}$ are presently underway to directly determine, or set a limit on, J for the present model system. If the oxygenated (*b*) solution is degassed with N_2, spectrum (*d*) results which is again similar to spectra (*a*) through (*c*), except for a slight increase in the $g_{\perp} = 2.1$ signal. Spectra (*e*) and (*f*) are for the second

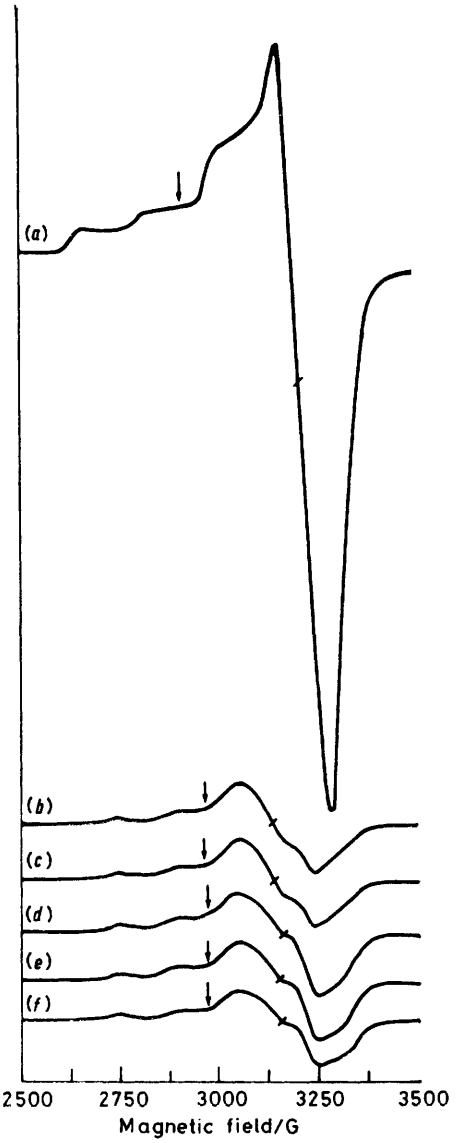

FIGURE 10 E.s.r. spectra for the copper complexes in dmso glasses at *ca.* 100 K. [Cu] = 10^{-3} mol dm^{-3} for all samples: (*a*) $[Cu^{II}(imep)]^{2+}$ (green solution); (*b*) $[Cu^{I}(imep)]^{+}$ (red solution; 2× actual intensity); (*c*) solution (*b*) after absorption of 0.5 : 1 mol O_2 : Cu (oxy of first cycle; green solution; 2× actual intensity); (*d*) solution (*c*) degassed with N_2 (deoxy of first cycle; red solution; 2× actual intensity); (*e*) solution (*d*) exposed to O_2 (oxy of second cycle; green solution; 2× actual intensity); (*f*) solution (*e*) degassed with N_2 (deoxy of second cycle; red solution; 2× actual intensity)

oxy/deoxy cycle and again there is no significant increase in detectable copper. From these results it is concluded that both the deoxy and oxy forms of $[Cu^{I}(imep)]^{+}$ are essentially diamagnetic species at 100 K and that the small spectral differences that occur upon oxy/-

deoxy cycling are due to additional small amounts of irreversibly oxidized Cu^{II}.

In summary, the spectroscopic, manometric, electrochemical, and *in situ* e.s.r. data reported here are all considerable evidence for establishing the $[Cu^{I}(imep)]^{+}$ cation as the first synthetic Cu^{I} oxygen carrier in solution. It is true, however, that many of these same results might also be adequately explained by ligand oxidation or other pathways involving cyclical oxidation to Cu^{II} (without stable O_2-adduct formation), followed by re-reduction to Cu^{I} in the absence of O_2. While we do not believe this to be the case, definitive evidence to the contrary must await the isolation and structuring of a dioxygen adduct. Effort in this direction, employing a variety of copper(I) substituted imep derivative compounds and other copper(I) unsymmetrical ligand systems (containing an imidazolyl and a pyridyl group) under a range of temperature and O_2-pressure conditions, is being intensely pursued.

We thank The Robert A. Welch Foundation for grants (to L. J. W. and K. M. K.), the National Science Foundation (L. J. W.), the National Institute of Health (K. M. K.), and the Petroleum Research Fund (L. J. W.) for support of this work. We are also indebted to Professor Robert Gagné for several rewarding discussions.

[9/1747 *Received*, 30*th October*, 1979]

REFERENCES

[1] J. M. Rifkind, in ' Inorganic Biochemistry,' ed. G. L. Eichhorn, Elsevier, Amsterdam, 1973, vol. 2, and refs. therein.
[2] J. P. Collman, *Accounts Chem. Res.*, 1977, **10**, 265; J. P. Collman, R. R. Gagné, T. R. Holbert, J. Marchon, and C. A. Reed, *J. Amer. Chem. Soc.*, 1973, **95**, 7868.
[3] T. K. Eccles, Stanford Synchrotron Radiation Laboratory Report No. 78/01, Stanford University, Stanford, California, 1978.
[4] A. R. Amudsen, J. Whelan, and B. Bosnich, *J. Amer. Chem. Soc.*, 1977, **99**, 6730.
[5] O. Warburg, in ' Heavy Metal Prosthetic Groups,' Oxford University Press, London, 1949.
[6] T. Nakamura and H. S. Mason, *Biochem. Biophys. Res. Comm.*, 1960, **3**, 297; J. F. Boas, J. R. Pilbrow, G. J. Troup, C. Moore, and T. D. Smith, *J. Chem. Soc.* (*A*), 1969, 965.
[7] J. S. Loehr, T. B. Freedman, and T. M. Loehr, *Biochem. Biophys. Res. Comm.*, 1974, **56**, 510; T. B. Freedman, S. Loehr, and T. M. Loehr, *J. Amer. Chem. Soc.*, 1976, **98**, 2809.
[8] H. B. Gray, in ' Bioinorganic Chemistry,' ed. R. F. Gould, American Chemical Society, Washington, 1971.
[9] H. A. Kuiper, R. Torensma, and E. F. J. van Bruggen, *European J. Biochem.*, 1976, **68**, 425; C. Bonaventura, B. Sullivan, J. Bonaventura, and S. Bourne, *Biochemistry*, 1974, **13**, 4784; L. Y. Fager and J. O. Alben, *ibid.*, 1972, **11**, 4786.
[10] A. J. M. Schoot Uiterkamp, *FEBS Letters*, 1972, **20**, 93.
[11] F. H. Jardine, *Adv. Inorg. Chem. Radiochem.*, 1975, **17**, 115.
[12] R. R. Gagné, J. L. Allison, R. S. Gall, and C. A. Koval, *J. Amer. Chem. Soc.*, 1977, **99**, 7170; R. R. Gagné, *ibid.*, 1976, **98**, 6709 and refs. therein.
[13] L. Graf and S. Fallar, *Experientia*, 1964, **20**, 46.
[14] E. Ochiai, *Inorg. Nuclear Chem. Letters*, 1973, **9**, 987.
[15] C. S. Arcus, J. L. Wilkinson, C. Mealli, T. J. Marks, and J. A. Ibers, *J. Amer. Chem. Soc.*, 1974, **96**, 7564.
[16] C. E. Kramer, G. Davies, R. B. Davis, and R. W. Slaven, *J.C.S. Chem. Comm.*, 1975, 606.
[17] J. E. Bulkowski, P. L. Burk, M. Ludmann, and J. A. Osborn, *J.C.S. Chem. Comm.*, 1977, 498.
[18] M. G. Simmons and L. J. Wilson, *J.C.S. Chem. Comm.*, 1978, 634.
[19] P. Hemmerich and C. Sigwart, *Experientia*, 1963, **19**, 488.
[20] W. W. Umbreit, R. H. Burris, and J. F. Stauffer, ' Manometric Techniques,' 4th edn., Burgess, Minneapolis, 1964.
[21] A. G. Zwart, *Biochim. Biophys. Acta*, 1952, **9**, 104.
[22] L. Vaska, *Science*, 1963, **140**, 809.
[23] R. C. Slade, A. A. G. Tomlinson, B. J. Hathaway, and D. E. Billing, *J. Chem. Soc.* (*A*), 1968, 61; P. C. Jain and E. C. Lingafelter, *J. Amer. Chem. Soc.*, 1967, **89**, 6131.
[24] M. Ciampolini and N. Nardi, *Inorg. Chem.*, 1966, **5**, 41.
[25] L. Morpurgo, R. Falcioni, and G. Ritilio, *Inorg. Chim. Acta*, 1978, **28**, L141.
[26] K. E. van Holde, *Biochemistry*, 1967, **6**, 93; E. Frieden, S. Osaki, and H. Kobayashi, *J. Gen. Phys.*, 1965, **49**, Pt. 2, 213.
[27] C. L. Merrill, J. M. Trantham, and L. J. Wilson, unpublished work.
[28] See for example, A. D. Zuberbuhler, ' Metal Ions in Biological Systems,' ed. H. Sigel, Dekker, New York, 1975, vol. 5, ch. 7.
[29] F. H. Jardine, *Adv. Inorg. Chem. Radiochem.*, 1975, **17**, 115.
[30] R. R. Gagné, R. S. Gall, G. C. Lisensky, R. E. Marsh, and L. M. Speltz, *Inorg. Chem.*, 1979, **18**, 771.
[31] R. S. Nicholson and I. Shain, *Analyt. Chem.*, 1964, **36**, 706.
[32] R. J. Sundberg and R. B. Martin, *Chem. Rev.*, 1974, **74**, 471; E. Ochiai, *J. Inorg. Nuclear Chem.*, 1975, **37**, 1503.
[33] R. J. Sundberg, R. F. Bryan, I. F. Taylor, and H. Taube, *J. Amer. Chem. Soc.*, 1974, **96**, 381; K. Schofield, ' Hetero-Aromatic Nitrogen Compounds. Pyrroles and Pyridines,' Plenum Press, New York, 1967, chs. 2 and 3.
[34] W. J. Eilbeck, F. Holms, G. G. Philips, and A. E. Vanderhill, *J. Chem. Soc.* (*A*), 1967, 1161; L. M. Epstein, D. K. Straub, and C. Maricondi, *Inorg. Chem.*, 1967, **16**, 1720; F. A. Walker, *J. Amer. Chem. Soc.*, 1973, **95**, 1150.
[35] J. B. Headridge, ' Electrochemical Techniques for Inorganic Chemists,' Academic Press, New York, 1969, p. 83.
[36] G. McLendon and M. Mason, *Inorg. Chem.*, 1978, **17**, 362; W. M. Coleman and L. T. Taylor, *Inorg. Chim. Acta*, 1978, **30**, L291.
[37] D. T. Sawyer and J. L. Roberts, jun., ' Experimental Electrochemistry for Chemists,' Wiley, New York, 1974, p. 172.
[38] K. F. Purcell and J. F. Kotz, ' Inorganic Chemistry,' W. B. Saunders, Philadelphia, 1977, p. 221.
[39] E. I. Solomon, D. M. Dooley, R. Wang, H. B. Gray, M. Cerdonio, F. Mogno, and G. L. Romani, *J. Amer. Chem. Soc.*, 1976, **98**, 1029; D. M. Dooley, R. A. Scott, J. Ellinghaus, E. I. Soloman, and H. B. Gray, *Proc. Nat. Acad. Sci. U.S.A.*, 1978, **75**, 3019.
[40] N. C. Eickman, R. S. Himmelwright, and E. I. Solomon, *Proc. Nat. Acad. Sci. U.S.A.*, 1979, **76**, 2094.